## Enhancing Gemcitabine Delivery in Mia-Paca-2 cells using a Combination of Rapid Short Ultrasound Pulse and Microbubbles

M.Sc. THESIS

# By ARNOLD BASUMATARY

2303171023



# DEPARTMENT OF BIOSCIENCES AND BIOMEDCIAL ENGINEERING

## INDIAN INSTITUTE OF TECHNOLOGY INDORE

**MAY 2025** 

## Enhancing Gemcitabine Delivery in Mia-Paca-2 cells using a Combination of Rapid Short Ultrasound Pulse and Microbubbles

## **A THESIS**

Submitted in partial fulfillment of the requirements for the award of the degree

of

**Master of Science** 

by

ARNOLD BASUMATARY

2303171023



# DEPARTMENT OF BIOSCIENCES AND BIOMEDCIAL ENGINEERING

## INDIAN INSTITUTE OF TECHNOLOGY INDORE

**MAY 2025** 



## INDIAN INSTITUTE OF TECHNOLOGY INDORE

## **CANDIDATE'S DECLARATION**

I hereby certify that the work which is being presented in the thesis entitled Enhancing Gemcitabine Delivery in Mia-Paca-2 cells using a Combination of Rapid Short Ultrasound Pulse and Microbubbles in the partial fulfilment of the requirements for the award of the degree of MASTER OF SCIENCE and submitted in the DEPARTMENT OF BIOSCIENCES AND BIOMEDICAL ENGINEERING, Indian Institute of Technology Indore, is an authentic record of my own work carried out during the time period from August 2023 of joining the M.Sc. program to May 2025. Thesis submission under the supervision of Dr. Lokesh Basavarajappa.

The matter presented in this thesis has not been submitted by me for the award of any other degree of this or any other institute.

Signature of the student with date (Mr. Arnold Basumatary)

This is to certify that the above statement made by the candidate is correct to the best of my/our knowledge.

Signature of the Supervisor of M.Sc. thesis

(Dr. Lokesh Basavarajappa)

Mr. Arnold Basumatary has successfully given his M.Sc. Oral Examination held on 06 May 2025.

Signature of Supervisor of M.Sc. thesis

Noce

Date: 20 05 2025

Convener, DPGC

Date: 20/05/2025

## **ACKNOWEDGEMENTS**

First and foremost, I would like to express my sincere gratitude to my supervisor, Dr. Lokesh Basavarajappa, for their invaluable guidance, constant support, and insightful feedback throughout the course of this research. Their expertise and encouragement have been instrumental in shaping this work.

I extend my heartfelt thanks to the faculty and staff of the Biosciences and Biomedical Engineering of Indian Institute of Technology Indore for providing the resources and a conducive research environment necessary for the completion of this thesis. Special thanks to Prof. Amit Kumar Lab for providing the Mia-Paca cell line, Dr. Hitendra Kumar and Dr. Sivaraj M Sundaram Lab for access to essential equipment and technical assistance.

I would also like to acknowledge the support of my colleagues and friends, whose camaraderie and discussions have greatly enriched my academic journey. Their moral support helped me stay motivated during the challenging phases of this work.

Finally, I am deeply grateful to my family for their unwavering love, patience, and encouragement, which have been the backbone of my perseverance and success.

#### **Abstract**

Pancreatic cancer remains one of the most lethal malignancies, with a 5-year survival rate below 10%, primarily due to late diagnosis, limited therapeutic options, and poor drug delivery. The tumor's dense fibrotic stroma, abnormal vasculature, and elevated interstitial pressure significantly hinder the effective penetration of chemotherapeutic agents such as gemcitabine hydrochloride (dFdC HCl). Previous studies have shown that ultrasound-mediated microbubble therapy can enhance drug delivery in solid tumors, including pancreatic cancer. For example, ultrasound combined with microbubble treatment has been utilized to enhance paclitaxel uptake in breast tumor models and to enhance dFdC HCl uptake, leading to tumor regression in pancreatic cancer xenografts. However, many of these approaches involved prolonged ultrasound exposure or high acoustic pressures, often leading to microbubble destruction and tissue damage, thus limiting reproducibility and clinical translation.

To address these limitations, our study evaluated the use of rapid short ultrasound pulse in combination with SonoVue microbubbles to enhance the delivery of dFdC HCl in MIA PaCa-2 pancreatic cancer cells. Cells were treated with increasing concentrations of dFdC HCl alone or in combination with ultrasound and microbubbles. Cell viability was assessed via MTT assay to find the IC<sub>50</sub> value of dFdC HCl drug. The membrane permeability was assessed with fluorescence images to find optimal microbubble concentration and ultrasound intensity by evaluating the uptake of Ethidium Homodimer-1 (EtHD-1). An increase in EtHD-1 uptake was observed with 10<sup>7</sup> microbubbles at mid-intensity (275V) and also with high-intensity ultrasound pulses (400V) in the absence of microbubbles. dFdC HCl displayed a dose-dependent cytotoxic effect, which was significantly enhanced by ultrasound exposure. The inclusion of 10<sup>7</sup> microbubble concentration further increased cytotoxicity, particularly at lower drug concentrations.

These findings suggest that rapid short ultrasound pulse, when paired with microbubbles, significantly improves dFdC HCl efficacy by

enhancing sonoporation and intracellular drug delivery. This minimally invasive and tunable approach holds promise for overcoming key drug delivery barriers in pancreatic cancer and merits further investigation in in-vivo models for potential clinical application.

## **Keywords:**

Pancreatic cancer, dFdC HCl, Ultrasound, Microbubbles, Sonoporation, Drug delivery,

## TABLE OF CONTENTS

	Page No.
I.	ACKNOWLEDGMENTSi
II.	ABSTRACTiii
III.	LIST OF FIGURESvii
IV.	ABBREVIATIONSxi
Chap	ter 1
1.	Introduction1
	1.1 Pancreatic Ductal Adenocarcinoma1
	1.2 Microbubbles1
	1.3. Ultrasound Microbubble Combination Therapy3
Chap	ter 2
2.	Objectives
Chap	ter 3
3.	Material and Methods9
	3.1 Materials
	3.2 Cell Culturing
	3.3 MTT Assay for Assessing dFdC HCl Cytotoxicity10
	3.4 Characterization of Microbubble Size Distribution11
	3.5 Ultrasound Treatment at Varying Intensities and
	Microbubble Concentrations11
	3.5.1 Development of an Ultrasound Therapy Setup11
	3.5.2 Microbubble Preparation
	3.5.3 EtDH-1 Cellular Uptake
	3.5.4 Fluorescence Imaging14
	3.5.5 Quantification of EtDH-1 Uptake14
	3.6 Enhancement of dFdC HCl Cytotoxicity using Combination
	of Ultrasound and Microbubble15
Chap	ter 4
4	Results and Discussion 19

4.1 MTT Assay of dFdC HCl19
4.2 Characterization of Microbubble Size Distribution20
4.3 EtDH-1 Cellular Uptake Experiment for Different
Ultrasound Intensities and Microbubble Concentrations21
4.4 MTT Assay to check Biocompatibility of Ultrasound
Microbubble Combination Therapy24
4.5 Enhanced Cytotoxicity of dFdC HCl via Combined mid-
Intensity Ultrasound with Microbubbles25
4.6 Enhanced Cytotoxicity of dFdC HCl via Combined high-
intensity Ultrasound with Microbubbles26
Chapter 5
5. Summary and Future prospects29
References

## LIST OF FIGURES

Figure 1	A) Schematic representation of a microbubble	Page No. 2
	showing its gas core and surrounding shell	
	composed of lipids, proteins, and polymers	
	with approximate thickness ranges. (B)	
	Microscopic image of the microbubbles,	
	captured at 60x magnification, demonstrating	
	their spherical morphology and polydispersity	
	in size.	
Figure 2	This diagram illustrates the two types of	Page No. 4
	cavitation induced by ultrasound waves:	
	inertial cavitation and stable cavitation. The	
	type of cavitation depends on the ultrasound	
	pressure relative to the cavitation threshold.	
	Inertial cavitation leads to microbubble	
	implosion and fragmentation, while stable	
	cavitation result in stable expansion and	
	compression.	
Figure 3	Picture showing 3D printed model parts utilized	Page No. 12
	to setup the ultrasound microbubble therapy	
	experiments	
Figure 4	Picture showing experimental setup of the	Page No. 12
	ultrasound microbubble combination therapy	
	experiment for EtDH-1 uptake.	
Figure 5	Diagrammatic workflow of EtDH-1 cellular	Page No. 15
	uptake experiment	
Figure 6	Picture showing experimental setup for dFdC	Page No. 16
	HCl delivery using ultrasound microbubble	
	combination experiment.	
Figure 7	Diagrammatic workflow of the ultrasound drug	Page No. 17
	delivery experiment performed to examine	
<u> </u>		1

	dFdC HCl cytotoxicity using combination of	
	ultrasound and microbubble	
Figure 8	MTT assay showing the effect of increasing	Page No. 19
	concentrations of dFdC HCl on the viability of	
	MIA PaCa-2 pancreatic cancer cells. Cells were	
	treated with 1-15 µg/mL of dFdC HCl for 48	
	hours. A dose-dependent reduction in cell	
	viability was observed, with significant	
	cytotoxicity at higher concentrations,	
	indicating the drug's effectiveness in inhibiting	
	pancreatic cancer cell growth. Data are	
	expressed as Mean $\pm$ SE.	
Figure 9	Representative microscopic images (A, B, and	Page No. 20
	C) of microbubbles captured from different	
	areas. Image processing techniques were	
	subsequently applied to these micrographs to	
	determine the size distribution of the	
	microbubble population.	
Figure 10	Histogram bars represent the number of	Page No. 20
	microbubbles within each size bin, showing a	
	distribution across 0–15 μm. The red dashed	
	line indicates a Gaussian fit, with a peak around	
	6-8 μm, highlighting the predominant size	
	range of the microbubble population	
Figure 11	Fluorescence microscopy images showing	Page No. 22
	calcein AM (green, live cells) and EtHD-1 (red,	
	membrane-compromised cells) staining after	
	treatment with varying ultrasound intensities	
	and microbubble concentrations.	
Figure 12	Bar graph showing the percentage of EtHD-1	Page No. 23
	uptake in MIA PaCa-2 cells following exposure	
	to low (red), mid (blue), and high (green)	
	intensity ultrasound pulses, with or without	

	microbubbles. Ctrl and MB represents	
	untreated cells and microbubbles, respectively.	
	EtHD-1 uptake indicates membrane	
	permeability induced by sonoporation.	
	Increased uptake was observed with higher	
	intensity ultrasound pulse, while microbubble	
	enhancement varied depending on the acoustic	
	condition. Data are expressed as mean ±	
	SE(N=3), (***p<0.0001).	
Figure 13	MTT assay results evaluating the	Page No. 24
	biocompatibility of ultrasound (US),	
	microbubbles (MB), and their combination (US	
	+ MB) on MIA PaCa-2 cell viability. Cells were	
	divided into four groups: untreated control, MB	
	alone, US alone, and US + MB. Viability was	
	measured 48 hours post-treatment and	
	expressed as a percentage relative to the	
	control. Data are presented as mean $\pm$ SE (N =	
	3).	
Figure 14	Effect of dFdC HCl on cell viability under three	Page No. 26
	conditions: dFdC HCl alone (red), dFdC HCl +	
	mid ultrasound intensity (blue), and dFdC HCl	
	+ mid ultrasound intensity + 10 <sup>7</sup> microbubbles	
	(green). All groups show dose-dependent	
	cytotoxicity, with enhanced effects in	
	ultrasound and microbubble-assisted	
	treatments, indicating improved drug delivery	
	via sonoporation. Data are expressed as mean ±	
	SE $(N=3)$ , $(*p<0.05)$ , $(**p<0.005)$ ,	
	(***p<0,0001).	
Figure 15	Effect of dFdC HCl on cell viability under three	Page No. 27
	conditions: dFdC HCl alone (red), dFdC HCl +	
	high ultrasound Intensity (blue), and dFdC HCl	

+ high ultrasound intensity  $+ 10^7$  microbubbles (green). All groups show dose-dependent cytotoxicity, with enhanced effects in ultrasound and microbubble-assisted treatments, indicating improved drug delivery via sonoporation. Data are expressed as mean  $\pm$  SE (N=3), (\*p<0.05), (\*\*p<0.005).

## **ABBREVIATIONS**

PDAC - Pancreatic ductal adenocarcinoma

PBS - Phosphate-buffered saline

DMEM - Dulbecco's modified eagle medium

FBS - Fetal bovine serum

BSL II - Biosafety level II

DMSO - Dimethyl sulfoxide

OD - Optical density

MTT - 3-(4,5-dimethylthiazol-2-yl)-2,5-diphenyltetrazolium bromide assay

dFdC HCl - Gemcitabine Hydrochloride

BBB - Blood-brain barrier

PRF - Pulse repetition frequency



## Chapter 1

## 1.Introduction

#### 1.1 Pancreatic Ductal Adenocarcinoma

Pancreatic cancer is a significant global health challenge, with an estimated 495,773 new cases and 466,003 deaths reported worldwide in 2020 [1]. Its five-year survival rate remains alarmingly low — often less than 10% — making it one of the deadliest malignancies. Among pancreatic cancers, pancreatic ductal adenocarcinoma (PDAC) is the most common and devastating form. It profoundly impacts patients, causing symptoms such as deep abdominal or back pain, significant weight loss, jaundice (yellowing of the skin and eyes), digestive problems, intense fatigue, and sudden loss of appetite. Many individuals also develop new-onset diabetes as the cancer disrupts the pancreas's ability to regulate blood sugar. As PDAC progresses, it often metastasizes to distant organs like the liver, lungs, and peritoneum, leading to additional complications such as fluid accumulation (ascites), worsening weakness, and eventual organ failure. The high mortality rate of PDAC is attributed to several factors, including late-stage diagnosis, the pancreas's anatomical complexity, and the cancer's resistance to treatment. Early-stage pancreatic cancer typically presents with vague, nonspecific symptoms, resulting in delayed detection and limited treatment options. Furthermore, the pancreas's deep location in the abdomen makes surgical resection technically challenging. The tumor microenvironment, characterized by a dense fibrotic stroma, hinders effective drug delivery and contributes to the failure of conventional chemotherapy. Additionally, the highly immunosuppressive nature of the PDAC microenvironment limits the success of immunotherapy, presenting further obstacles to improving patient outcomes [2].

### 1.2 Microbubbles

Microbubbles are critical tools in ultrasound-based imaging and drug delivery due to their unique structural and acoustic properties. They are meticulously engineered to maximize stability and functionality in biological systems. The schematic microscope view of microbubble is show in figure-1. The core typically consists of inert gases such as perfluorocarbon or sulfur hexafluoride, selected for their low solubility in blood, thereby enhancing circulation stability. Encasing the gas core is a stabilizing shell composed of proteins, polymers, or phospholipids, designed to mitigate surface tension and prevent premature collapse [3, [4, 5, 6]. Microbubbles generally range from 1 to 10 µm in diameter, a size that permits safe transit through the microvasculature. Structurally analogous to red blood cells, microbubbles can also circulate freely within capillary networks. These microbubbles undergo cyclic expansion and contraction upon ultrasound exposure. This behaviour enhances acoustic backscatter and facilitates localized drug release, rendering them highly effective vehicles for advanced therapeutic applications [7, 8, 9,10]. Regulatory guidelines, such as those established by the U.S. Food and Drug Administration (FDA), stipulate that clinical microbubble preparations should fall within a 1.1–3.3 µm range, with no individual microbubble exceeding 20 µm [11, 12, 13]. For biomedical applications, maintaining a diameter below 10 µm is considered optimal [12, 14, 15].

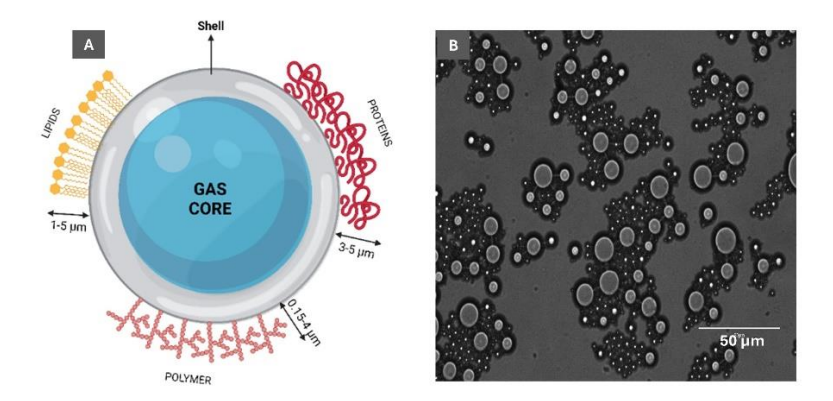


Figure-1: A) Schematic representation of a microbubble showing its gas core and surrounding shell composed of lipids, proteins, and polymers with approximate thickness ranges. (B) Microscopic image of the microbubbles, captured at 60x magnification, demonstrating their spherical morphology and polydispersity in size.

Although sonication remains a common fabrication method, it often produces a polydisperse population, with some microbubbles reaching diameters of up to 50  $\mu$ m. Consequently, additional size refinement techniques, including flotation, differential centrifugation, or acoustic sorting, are employed to achieve a narrower distribution, typically within the preferred 4–6  $\mu$ m range [12].

## 1.3. Ultrasound Microbubble Combination Therapy

Ultrasound and microbubble combination therapy has emerged as a novel and promising approach to overcoming this barrier. Ultrasound waves interacting with gas-filled microbubbles induce oscillations, where bubbles expand during low-pressure phases and contract during high-pressure phases—a phenomenon known as **cavitation** [3, 16]. This mechanical activity increases cellular permeability by forming transient pores or disrupting intercellular junctions, thereby enhancing the delivery of therapeutic compounds to target tissues. This process, termed **bubble-based sonoporation** [4, 5, 11]. It leverages cavitation to facilitate drug transport across vascular barriers and has shown promise in treating cancers, cardiovascular diseases, and in opening the blood-brain barrier (BBB) [12, 13].

Effective bubble-based sonoporation relies on optimising ultrasound parameters such as **frequency**, **acoustic pressure** (intensity), **pulse duration**, and **duty cycle**. Depending on the strength acoustic pressure, ultrasound waves can be classified as either high-intensity or low-intensity, each producing distinct microbubble dynamics and biological outcomes:

• High-intensity ultrasound waves induce inertial cavitation, where microbubbles undergo violent expansion (often more than twice their original radius) followed by rapid collapse [3, 11, 14]. This collapse generates localised shockwaves, microjets, and microstreaming, resulting in transient pore formation and localised heating. These effects enhance drug uptake, especially in multidrug-resistant cells [15, 17]. High-intensity ultrasound is clinically used in tumor ablation and kidney stone fragmentation. Additionally, it can promote the formation of

reactive oxygen species, which may modulate drug resistance pathways and enhance therapeutic efficacy [3, 11, 14].

• Low-intensity ultrasound waves, in contrast, promote stable cavitation, where microbubbles oscillate near their equilibrium radius without collapsing or generating substantial heat [18]. These linear and nonlinear oscillations—determined by ultrasound parameters and bubble mechanical properties—produce shear-field stress and localised fluid microstreaming. The resulting shear forces on the cell membrane can open transient pores and increase convective transport, facilitating the extravascular movement of macromolecules [11, 19, 20]. This mechanism significantly improves intercellular and paracellular transport, enhancing the therapeutic reach of bioactive agents [11, 21, 22].

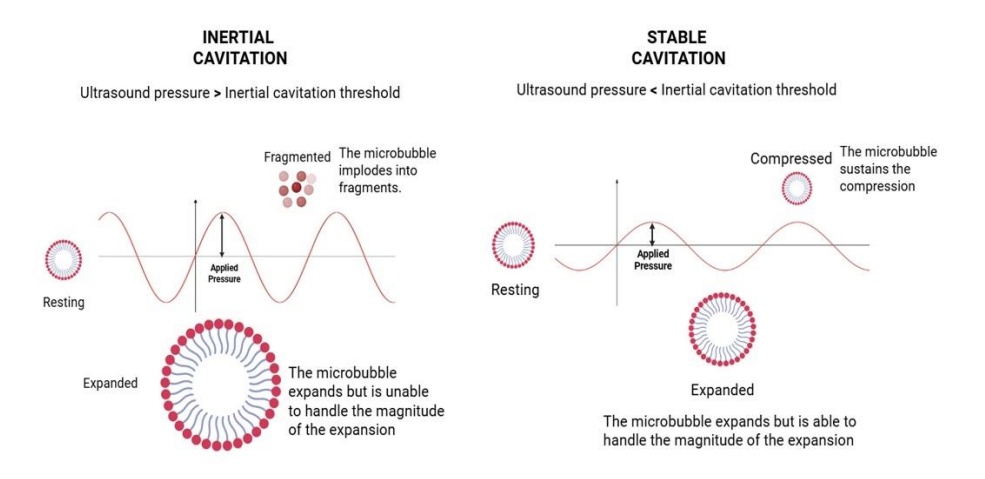


Figure-2: This diagram illustrates the two types of cavitation induced by ultrasound waves: inertial cavitation and stable cavitation. The type of cavitation depends on the ultrasound pressure relative to the cavitation threshold. Inertial cavitation leads to microbubble implosion and fragmentation, while stable cavitation result in stable expansion and compression. Created using Bio-render.

Both high- and low-intensity ultrasound, combined with microbubbles, have demonstrated substantial **preclinical and clinical efficacy** in oncology. These methods have been successfully applied to conditions such as breast fibroadenomas, hepatocellular carcinoma, and oral

cancers in experimental models, as well as pancreatic ductal adenocarcinoma in human patients. Continued advancements in **microbubble engineering** are enabling increasingly targeted and controlled drug delivery to tumors, presenting a promising frontier for **precision cancer therapy.** 

Traditionally, long-pulse ultrasound sequences were employed to induce cavitation for therapeutic purposes. However, these protocols have significant limitations. Prolonged exposure often leads to rapid microbubble destruction, diminishing their availability for sustained therapeutic action. Additionally, such sequences reduce overall treatment efficacy and increase the risk of thermal and mechanical damage to adjacent healthy tissues [23, 24]. These risks are particularly concerning in sensitive applications, such as opening the BBB, where precision and safety are paramount to avoid unintended neurological damage [25, 26].

To address these limitations, **rapid short-sequence ultrasound pulses** have been developed recently. These shorter pulses minimize microbubble destruction, enabling repeated dosing while reducing the risk of collateral tissue damage. The intense acoustic forces generated by rapid pulses improve drug penetration into tumor tissues and allow for precise control over microbubble behavior, optimizing therapeutic outcomes. This approach has already shown promise in safely and effectively opening the BBB and is now being investigated for its potential in other treatments [25, 26].

In this study, we aim to evaluate the efficacy of rapid short-sequence ultrasound pulses in enhancing the delivery and therapeutic impact of dFdC HCl, a third-generation chemotherapeutic agent, in MIA PaCa-2 cells, a model of pancreatic ductal adenocarcinoma using Sonovue microbubble. By leveraging this innovative strategy, we seek to overcome the challenges posed by drug resistance and limited therapeutic delivery in pancreatic cancer, advancing the development of more effective treatment modalities.

## Chapter 2

## 2. Objectives

- 1. To determine the half-maximal inhibitory concentration (IC<sub>50</sub>) of dFdC HCl in MIA PaCa-2 pancreatic cancer cells by evaluating its dose-dependent cytotoxic effects using an MTT assay, thereby establishing a baseline drug sensitivity profile for subsequent therapeutic enhancement studies involving ultrasound and microbubble-mediated delivery.
- 2. To identify and utilize the optimal combination of microbubble concentration and ultrasound intensity that maximizes dFdC HCl uptake in MIA PaCa-2 pancreatic cancer cells, by assessing membrane permeability and intracellular delivery efficiency through EtHD-1 uptake and fluorescence-based imaging.
- 3. To evaluate the enhancement of dFdC HCl uptake and cytotoxicity in MIA PaCa-2 pancreatic cancer cells using the optimized combination of microbubble concentration and ultrasound intensity, with the aim of maximizing therapeutic efficacy through ultrasound-mediated sonoporation.

## Chapter 3

## 3. Materials and Methods

#### 3.1 Materials

Cell line - MIA PaCa-2 is a human pancreatic cancer cell line, Pancreatic carcinoma, epithelial-like morphology.

Chemicals- DMEM, FBS, Trypsin, Trypan Blue, Antibiotic/Antimycotic (Penicillin, Streptomycin/ Amphotericin B), PBS, NaCl (Sodium chloride), KCl (Potassium chloride), Na<sub>2</sub>HPO<sub>4</sub> (Disodium phosphate, anhydrous), KH<sub>2</sub>PO<sub>4</sub> (Monopotassium phosphate, Calcien AM, EtDH-1, Propidium Iodide (PI), DMSO (Dimethyl Sulfoxide), Microbubble (Sonovue), 0.9% NaCl Saline Solution.

Equipments – Biosafety level II (BSL II), Fluorescence Microscope (Thermofisher EVOS 5000), CO<sub>2</sub> Incubator, Density Gradient Centrifuge, Phase Contrast Microscope, Water Bath, UV Plate Reader, Ultrasound Pulser Receiver.

Software- AutoDesk Fusion 360 ®, ImageJ ®

All the cell culture supplies were purchased from Sigma and Hi-Media, the Sonovue microbubble were purchased from Bracco, and the Mia-Paca 2 cells were received from Prof. Amit Kumar Lab.

#### 3.2 Cell Culturing

The Mia-Paca 2 cell line were verified to be free of contamination and authenticated prior to use. The cell was maintained in DMEM high glucose supplemented with 5% FBS and 1% Antibiotic/Antimycotic (penicillin streptomycin and Amphotericin B). Cells were cultured in 25 mm<sup>2</sup> tissue culture flasks at seeding density 5 × 10<sup>5</sup> cells/cm<sup>2</sup>. Cultures were incubated at 37°C in a humidified atmosphere with 5% CO<sub>2</sub>. Medium was replaced every 2–3 days depending on the cell confluency to maintain cell viability. When cells reached 70-80% confluence, they were passaged. The medium was aspirated, and cells were washed with sterile PBS. Cells were detached using 0.25% trypsin-EDTA, and the reaction was quenched by adding 3 times the volume of complete medium. The cell suspension was centrifuged at 1100 rpm for 4 minutes, and the pellet was resuspended in a fresh medium. Cells were passaged at a ratio of 1:2 for continued culture and sterility was maintained throughout the culture process by performing all procedures in a biosafety level II (BSL II).

## 3.3 MTT Assay for Assessing dFdC HCl Cytotoxicity

The MTT assay was employed to evaluate the cytotoxic effects of dFdC HCl by measuring cell viability and proliferation over time. Cells were seeded into a 96-well plate at a density of 5,000 cells per well and allowed to adhere for 12 hours. Subsequently, cells were treated with varying concentrations of dFdC HCl (ranging from 1  $\mu$ g/mL to 15  $\mu$ g/mL) and incubated for 48 hours to assess drug-induced cytotoxicity.

Following treatment, 100  $\mu$ L of MTT solution (0.5 mg/mL in culture medium) was added to each well and incubated for 3 hours at 37°C. During this period, mitochondrial dehydrogenase in viable cells reduced the yellow MTT reagent to insoluble purple formazan crystals. After incubation, the culture medium was carefully removed, and the formazan crystals were solubilized by adding 100  $\mu$ L of DMSO to each well.

Absorbance was measured at 570 nm using a microplate reader. The OD values obtained were directly proportional to the number of viable cells.

Cell viability percentages were calculated based on the OD readings, and the IC<sub>50</sub> value of dFdC HCl was determined using the following formula:

% Viability = (Mean OD of sample / Mean OD of control) x 100 (Eq-1)

#### 3.4 Characterization of Microbubble Size Distribution

Commercially available SonoVue microbubbles were reconstituted as per manufacturer instructions. The suspension was gently agitated to ensure uniform distribution before analysis. A small volume of the microbubble suspension was diluted with PBS to reduce overlap and improve visualization under the microscope. A drop of the diluted microbubble suspension was placed on a clean glass slide, covered with a coverslip, and immediately imaged using an optical microscope at 60× magnification. Multiple fields were captured to ensure representative sampling. Images were analyzed using ImageJ software ®. The 'Analyze Particles' function was used to measure the diameter of individual microbubbles after appropriate thresholding and calibration. The measured diameters were compiled to generate a size distribution plot. A Histogram plot was constructed to visualize the frequency and spread of microbubble diameters, highlighting the median and interquartile range.

## 3.5 Ultrasound Treatment at Varying Intensities and Microbubble Concentrations

## 3.5.1 Development of an Ultrasound Therapy Setup

A custom design was made using Autodesk software and using a 3D printer (Kobra 2 Neo, Anycubic). The 3D printed parts of the setup are shown in **Figure 3**. This setup was used to ensure precise delivery of ultrasound waves to cell cultures. The apparatus consisted of a hollow base filled with water for acoustic coupling. The culture plate was placed on an opening in the lid to allow the culture medium to remain in contact with the water. A cone-shaped housing for the ultrasound transducer extended into the culture plate, with its opening sealed by a thin, water-

retaining membrane to isolate the transducer's water from the culture medium.

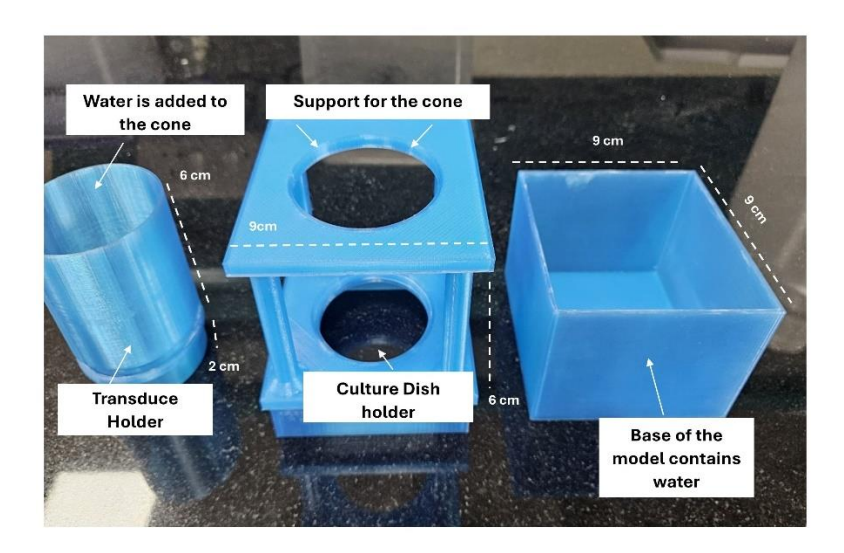


Figure-3: Picture showing 3D printed model parts utilized to setup the ultrasound microbubble therapy experiments

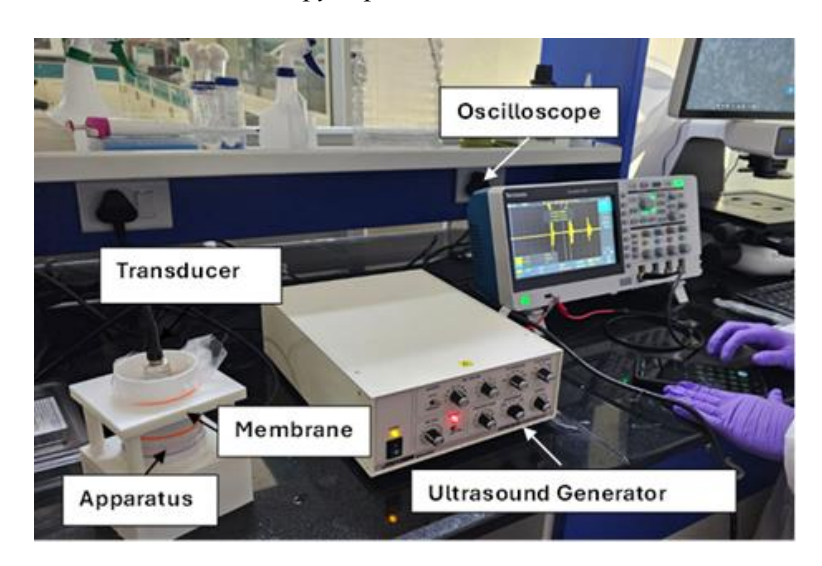


Figure-4: Picture showing experimental setup of the ultrasound microbubble combination therapy experiment for EtDH-1 uptake.

The ultrasound therapy was delivered using an ultrasonics pulse-receiver (DPR300, JSR Ultrasonics, USA) connected to a single element unfocused transducer. The operating frequency of the transducer was 1 MHz. The transducer was secured in the conical housing of the apparatus and fully submerged in water for consistent acoustic coupling.

The ultrasound parameters used during the therapy were as follows:

Pulse repetition frequency: 1 kHz

Pulse amplitude: Low-intensity (200 V), Mid-intensity (275 V), and High-intensity (400 V).

Pulse Duration: 150 µs

Exposure Time: 5 minutes per treatment session

### 3.5.2 Microbubble Preparation

SonoVue microbubbles, composed of a lipid shell encapsulating sulfur hexafluoride gas. A single vial of SonoVue was reconstituted in 5 mL of 0.9% saline solution. The resulting microbubble suspension was transferred to a 15 mL falcon tube and agitated vigorously for 20 seconds to promote microbubble formation. This process yielded microbubbles with an average diameter of approximately 7 µm.

The prepared solution contained an estimated 100 million microbubbles per milliliter. Various microbubble concentrations were tested to perform a dose-response study and different intensity of ultrasound was used to optimize the microbubble concentration.

#### 3.5.3 EtDH-1 Cellular Uptake

For this experimental assay, cells were seeded into 60 mm culture dishes, at a density of (specific density, e.g.,  $5 \times 10^5$  cells per well). Cells were allowed to adhere before proceeding with subsequent treatments or analyses. Cell morphology was monitored regularly using an inverted light microscope (Thermo Fisher EVOS 5000) to ensure consistent growth and absence of contamination. Sterility was maintained throughout the culture process by performing all procedures in a biosafety cabinet. and divided into experimental groups: untreated cells, ultrasound-treated cells, microbubble-only cells, and cells treated with both ultrasound and microbubbles. Prior to treatment, the spent culture medium was aspirated, and the cells were washed thoroughly with PBS. Fresh culture medium (5 mL) was then added to each plate, followed by

1 mL of a 2  $\mu$ M EtDH-1 and Calcien AM solution after the treatment. For the ultrasound + microbubble group, different volumes of the microbubble solution were added and were introduced to different intensity of ultrasound as specified in the experimental protocol.

The plates were placed on a custom-designed apparatus filled with deionized water, ensuring the ultrasound transducer was fully submerged and that water levels remained consistent throughout the experiment. The setup is shown in figure 5. The culture plates were positioned on the apparatus lid, allowing direct contact between the plate base, the water-filled hollow chamber, and the transducer cone for optimal acoustic coupling. Ultrasound treatment was applied for 5 minutes using the specified parameters. Following insonation, the plates were incubated in the dark for 30 minutes. After incubation, the media containing the staining solution and microbubbles was aspirated, and the plates were washed with PBS to remove residual stain. Fluorescence imaging was then performed to detect red fluorescence, indicative of EtDH-1 uptake, as a measure of cell membrane permeability.

#### 3.5.4 Fluorescence Imaging

Images were captured using fluorescence microscope (Thermo Fisher EVOS 5000) using three different filter. A green filter was used to visualize cells stained with Calcein, which labels live cells, while a red filter was used to image cells stained with EtDH-1, which identifies dead or membrane-compromised cells. The trans filter was used to obtain a greyscale image. Appropriate exposure settings were adjusted for each channel to optimize signal detection and minimize background noise. The images were later processed and analyzed to quantify live and dead cell populations.

#### 3.5.5 Quantification of EtDH-1 Uptake

The acquired images containing stained cells were analyzed using the built-in image processing software in the fluorescence microscope. Appropriate parameters, including threshold intensity and size filters, were set to accurately identify and count cells stained with Calcein

(green, live cells) and EtDH-1 (red, dead cells). After automated counting, the data were exported to an Excel spreadsheet for further analysis. The ratio of dead to live cells was then calculated using the following formula:

EtDH-1 Uptake (%) = (No. of Cells Stained Red / No. of Cells-Stained Green) x 100.....(Eq-2)

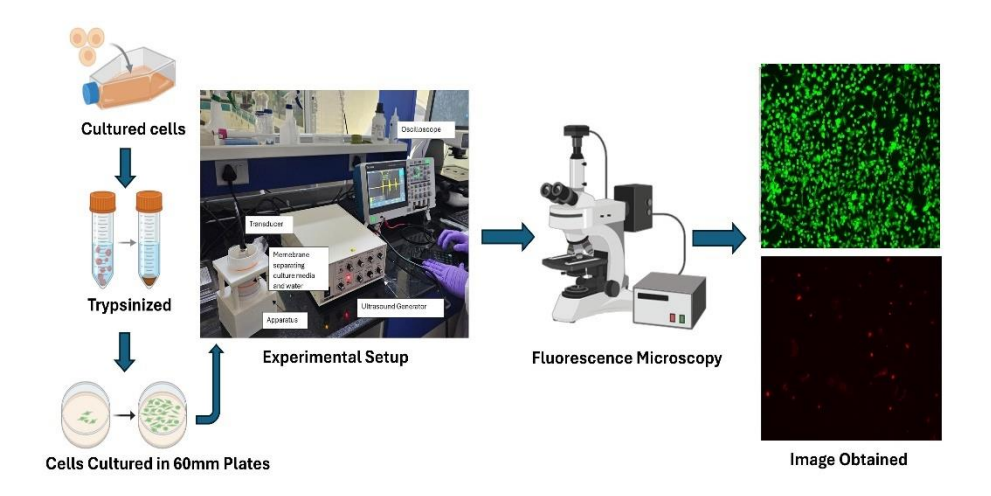


Figure-5: Diagrammatic workflow of EtDH-1 cellular uptake experiment

# 3.6 Enhancement of dFdC HCl Cytotoxicity using Combination of Ultrasound and Microbubble

Based on the MTT assay results, the optimal drug concentration was determined. Additionally, Calcien AM and EtDH-1 staining was used to optimize the microbubble concentration and ultrasound intensity parameters. From this optimization, a microbubble concentration of 10<sup>7</sup> and two ultrasound intensity levels (mid and high) at a pulse repetition frequency (PRF) of 1 kHz were selected for further experiments. The experiment was designed to compare different treatment groups: dFdC HCl only, dFdC HCl + Ultrasound, and Ultrasound + Microbubble + dFdC HCl. Furthermore, the same setup was used to evaluate the cellular compatibility and potential cytotoxic effects of Ultrasound alone, Microbubbles alone, and the combined Ultrasound–Microbubble treatment on MIA PaCa-2 cells.

The experimental setup used for treating cell-lines is shown in Figure 6. To ensure consistency, the initial setup was adjusted the cells were collected in a falcon tube then the falcon tube and the ultrasound transducer were submerged in a chamber containing water the falcon and the transducer are held into place using burette stands.

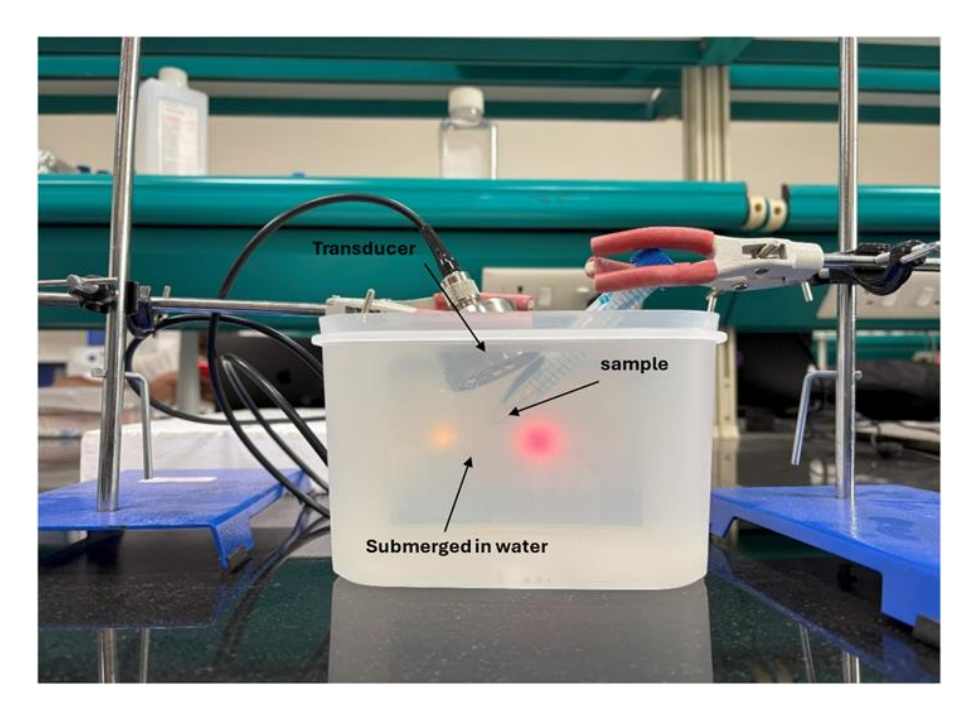


Figure-6: Picture showing experimental setup for dFdC HCl delivery using ultrasound microbubble combination experiment.

Cells are trypsinized, counted, and diluted to ensure each well in all groups contained 10,000 cells. The cells were then pelleted and resuspended in Falcon tubes according to their respective treatment conditions.

- **dFdC HCl group**: Cells were resuspended in fresh media containing dFdC HCl at different concentrations.
- **dFdC HCl** + **Ultrasound group**: Cells were resuspended in fresh media containing dFdC HCl at different concentrations and then exposed to ultrasound (mid-intensity, high-intensity at 1kHz pulse repetition frequency (PRF).
- dFdC HCl + Ultrasound + Micorbubble: Cells were pelleted and resuspended in fresh media containing dFdC HCl along with

microbubbles at a concentration of 10<sup>7</sup>. This suspension was then subjected to ultrasound exposure (mid-intensity and high intensity at 1kHz PRF).

After ultrasound treatment, the cells were seeded into a 96-well plate and incubated for 48 hours. Following incubation, the MTT assay was performed to assess cell viability and compare the effects of different treatment conditions.

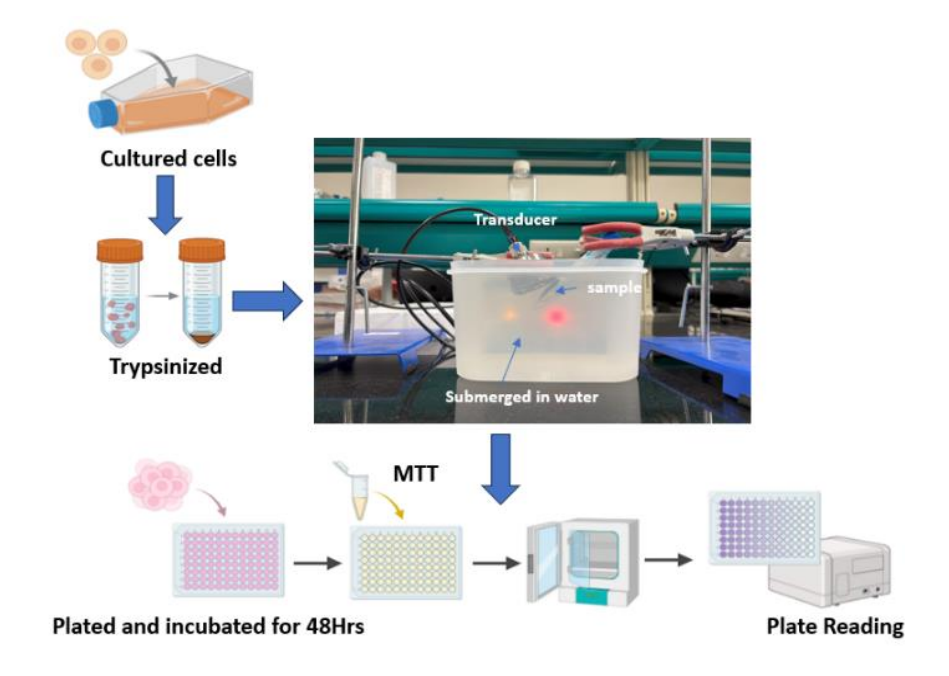


Figure-7: Diagrammatic workflow of the ultrasound drug delivery experiment performed to examine dFdC HCl cytotoxicity using combination of ultrasound and microbubble

## Chapter 4

## 4. Result and Discussion

### 4.1 MTT Assay of dFdC HCl

The MTT assay results shown in the **figure 8** illustrate the dose-dependent cytotoxic effects of dFdC HCl on MIA PaCa-2 pancreatic cancer cells. As the concentration of dFdC HCl increased from 1  $\mu$ g/mL to 15  $\mu$ g/mL, a progressive decline in cell viability was observed.

At the lowest tested concentration (1  $\mu$ g/mL), a moderate reduction in cell viability was noted compared to the untreated control, indicating initial sensitivity of the cells to the chemotherapeutic agent. As the concentration was increased to  $5 \mu$ g/mL and  $10 \mu$ g/mL, the viability further declined, reflecting enhanced cytotoxicity with higher drug exposure. At  $15 \mu$ g/mL, the cell viability dropped to its lowest point 51% in this experiment, suggesting that the therapeutic threshold had been surpassed and the cells were experiencing significant metabolic inhibition and death.

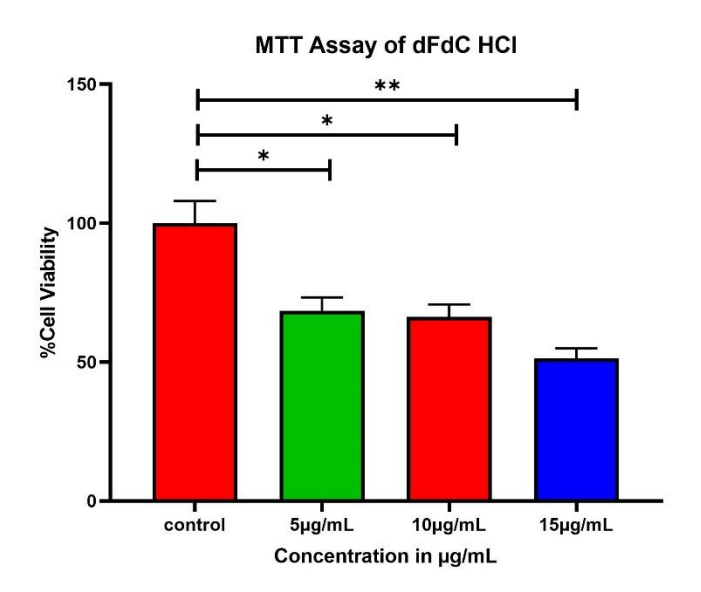


Figure-8: MTT assay showing the effect of increasing concentrations of dFdC HCl on the viability of MIA PaCa-2 pancreatic cancer cells. Cells were treated with  $1-15 \mu g/mL$  of dFdC HCl for 48 hours. A dose-dependent reduction in cell viability was observed, with significant cytotoxicity at higher concentrations, indicating the drug's effectiveness in inhibiting pancreatic cancer cell growth. Data are expressed as Mean  $\pm$  SE (N=3); (\*p <0.05) (\*\*p<0.005).

#### 4.2 Characterization of Microbubble Size Distribution

Representative microscopic images of microbubbles captured at 60x magnification are shown in **figure 9**. The images were processed in Image J software to estimate the size distribution of the microbubble population. The histogram plot in **figure 10** illustrates the size distribution of microbubbles used in this study, with diameters measured in micrometres. Most microbubbles fall within the 5–10 μm range, with a mean diameter centred around 6-8 μm.

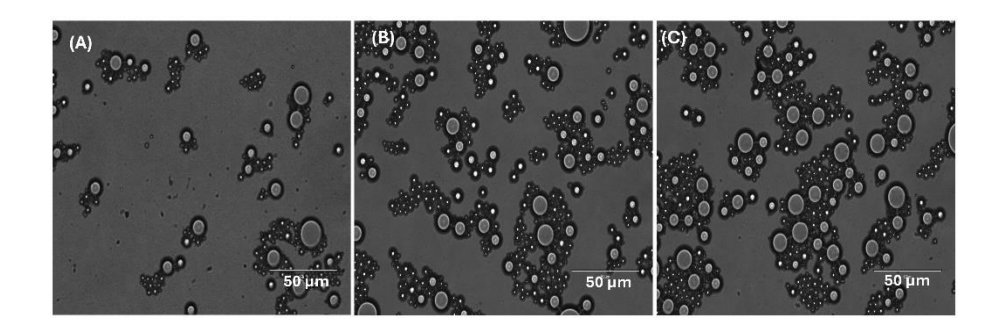


Figure-9: Representative microscopic images (A, B, and C) of microbubbles captured from different areas. Image processing techniques were subsequently applied to these micrographs to determine the size distribution of the microbubble population.

## Frequency distribution of Microbubble Size

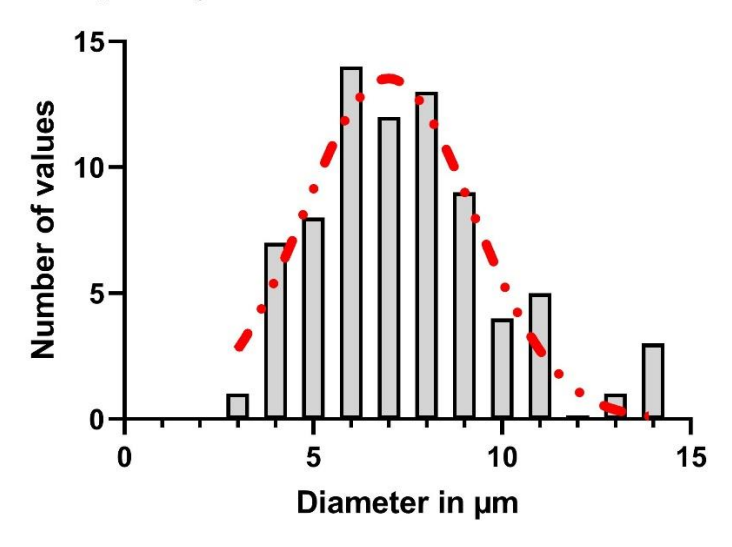


Figure-10: Histogram bars represent the number of microbubbles within each size bin, showing a distribution across 0– $15 \mu m$ . The red dashed line indicates a Gaussian fit, with a peak around 6- $8 \mu m$ , highlighting the predominant size range of the microbubble population.

This size range is appropriate for effective ultrasound-mediated cavitation, ensuring vascular compatibility and efficient oscillation under acoustic stimulation. The narrow spread and symmetric distribution suggest consistent microbubble formulation, which is critical for reproducibility and minimizing variability in ultrasound-microbubble interaction studies. Importantly, microbubbles within this size range are small enough to navigate through capillaries yet large enough to undergo stable cavitation, making them ideal candidates for drug delivery applications via sonoporation.

# 4.3 EtDH-1 Cellular Uptake Experiment for Different Ultrasound Intensities and Microbubble Concentrations

**Figure 11** shows the impact of varying ultrasound intensities and microbubble concentrations on EtDH-1 Cellular uptake by cell, which was evaluated using Calcein AM (green, live cells) and EtHD-1 (red, dead) staining. Control samples showed negligible EtHD-1 uptake with minimal EtHD-1 signal. Ultrasound alone induced a slight increase in EtDH-1 Cellular uptake, which became more pronounced with increasing intensity. The combination of ultrasound and microbubbles significantly enhanced membrane disruption and EtHD-1 Cellular uptake, particularly at mid-intensity ultrasound pulse with 10<sup>7</sup> microbubbles. At high-intensity ultrasound pulse, a clear intensity-dependent effect was observed even in the absence of microbubbles. The images were further analysed quantitatively, and the data were presented as a bar graph to confirm the observed trends.

The **figure 12** is a graphical representation of the effect of varying ultrasound intensities and microbubble concentrations on EtHD-1 Cellular uptake, an indicator of membrane permeability. As expected, control cells showed negligible EtHD-1 uptake, reflecting intact membrane integrity. Across all three ultrasound intensities—low (red), mid (blue), and high (green)—a marked increase in EtHD-1 uptake was observed compared to the control, confirming that ultrasound exposure enhances cell membrane permeability via sonoporation. This was

ascertained using the images that were obtained from fluorescence microscopy.

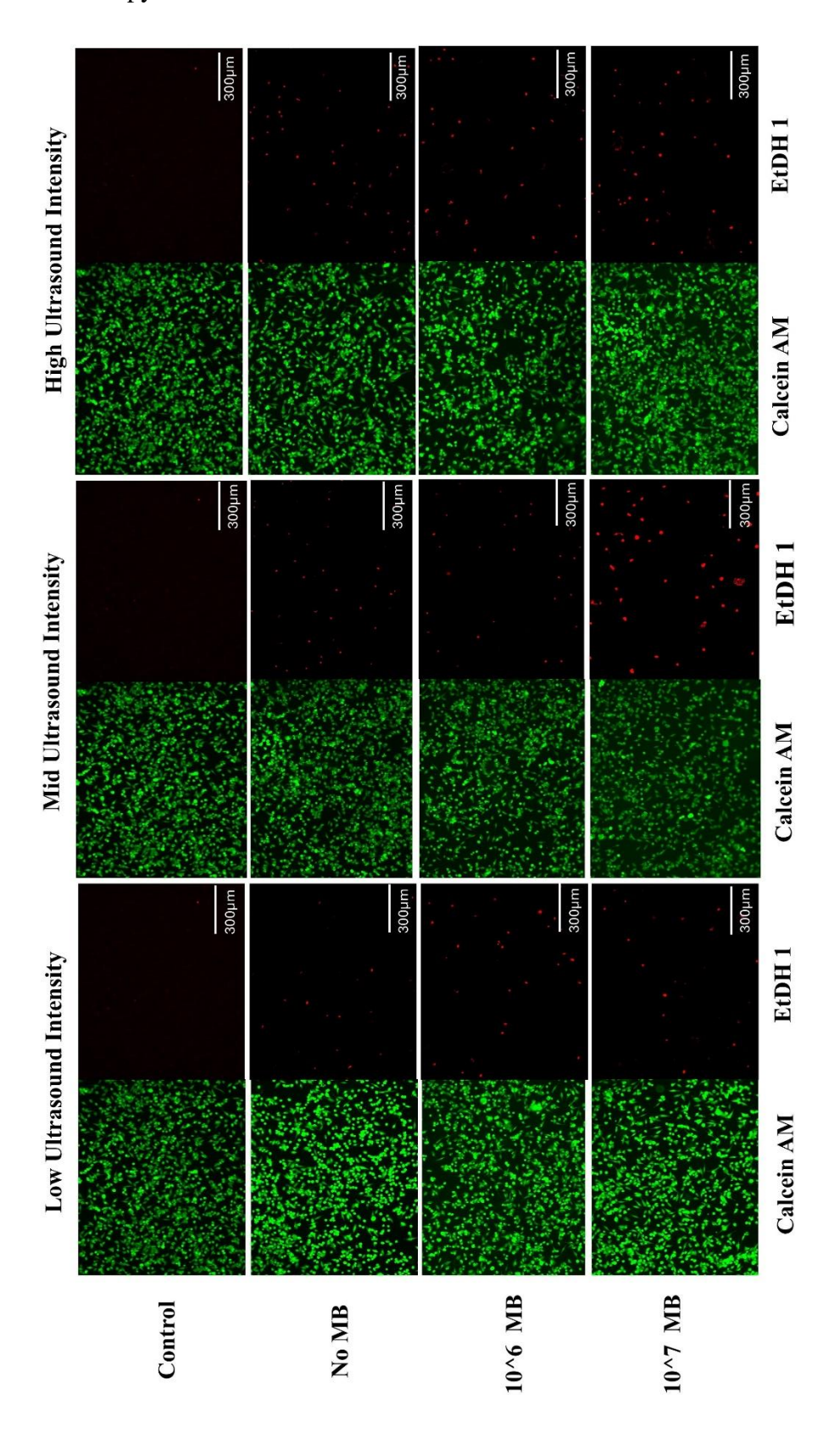


Figure-11: Fluorescence microscopy images showing calcein AM (green, live cells) and EtHD-1 (red, membranecompromised cells) staining after treatment with varying ultrasound intensity pulses and microbubble concentrations.

#### **EtHD 1 Cellulare Uptake**

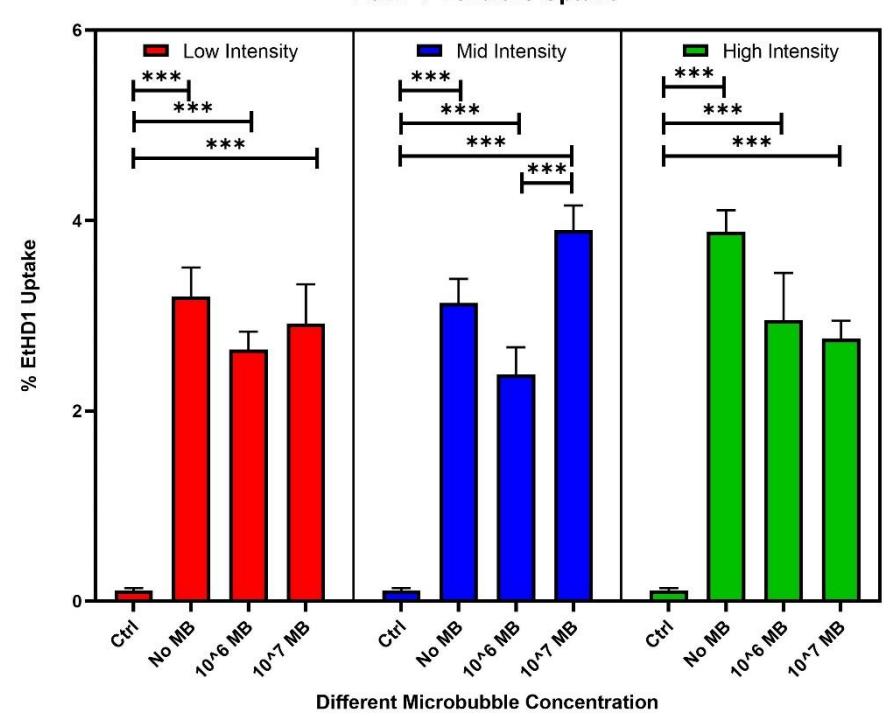


Figure-12: Bar graph showing the percentage of EtHD-1 uptake in MIA PaCa-2 cells following exposure to low (red), mid (blue), and high (green) intensity ultrasound pulses, with or without microbubbles. Ctrl and MB represents untreated cells and microbubbles, respectively. EtHD-1 uptake indicates membrane permeability induced by sonoporation. Increased uptake was observed with higher intensity ultrasound pulse, while microbubble enhancement varied depending on the acoustic condition. Data are expressed as  $mean \pm SE(N=3)$ , (\*\*\*p<0.0001).

At low intensity ultrasound pulse, EtHD-1 uptake was modest and relatively unaffected by microbubble concentration, indicating limited cavitation effects at this power level. In contrast, mid-intensity ultrasound pulse produced a more variable response: while 10<sup>7</sup> microbubble concentration yielded the highest uptake within this group, the enhancement over ultrasound alone (no microbubble) was moderate. At high intensity ultrasound pulse, EtHD-1 uptake peaked with ultrasound alone (no microbubble), suggesting that excessive intensity might lead to microbubble destruction or reduced stability, thereby diminishing their enhancing effect. The addition of 10<sup>6</sup> and 10<sup>7</sup> microbubble at high intensity did not further increase uptake and in fact showed slightly reduced values compared to ultrasound alone.

These results imply that while ultrasound is effective in promoting membrane permeabilization, the benefits of microbubble addition are highly dependent on acoustic conditions. An optimal balance is needed to achieve stable cavitation without inducing premature microbubble destruction. Fine-tuning parameters like pulse length, frequency, and PRF further improve delivery outcomes in sonoporation-based therapeutic strategies.

# 4.4 MTT Assay to Check Biocompatibility of Ultrasound Microbubble Combination Therapy

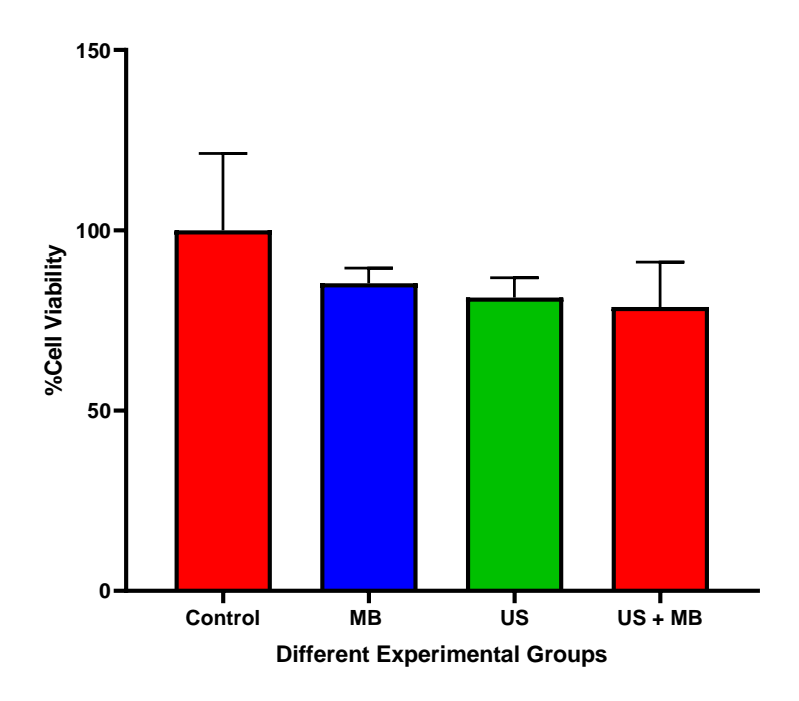


Figure-13: MTT assay results evaluating the biocompatibility of ultrasound (US), microbubbles (MB), and their combination (US + MB) on MIA PaCa-2 cell viability. Cells were divided into four groups: untreated control, MB alone, US alone, and US + MB. Viability was measured 48 hours post-treatment and expressed as a percentage relative to the control. Data are presented as mean  $\pm$  SE (N = 3); p<0.05.

Figure 13 presents the results of the MTT assay conducted to assess the biocompatibility of high-intensity ultrasound, microbubbles, and their combination on MIA PaCa-2 cell viability. The control group, consisting of untreated cells, exhibited the highest viability (~100%), indicating healthy and unaffected cells under standard culture conditions. Cells

exposed to microbubbles alone or ultrasound alone showed a moderate decrease in viability (~85%), suggesting mild stress or physical disruption—likely due to membrane interactions from microbubbles or mechanical effects of high-intensity ultrasound. Importantly, the group treated with the combination of ultrasound and microbubbles demonstrated the lowest viability (~80%) among all groups. However, this reduction was not significant when compared to the control, the combined treatment indicating that retains acceptable biocompatibility and can be considered safe for further therapeutic application.

## 4.5 Enhanced Cytotoxicity of dFdC HCl via Combined Mid Intensity Ultrasound with Microbubbles

**Figure 14** illustrates the effects of dFdC HCl treatment—administered alone or in combination with mid-intensity ultrasound, with or without microbubbles—on MIA PaCa-2 cell viability across increasing drug concentrations (5, 10, and 15 μg/mL). Treatment with dFdC HCl alone (red bars) induced a clear dose-dependent decrease in cell viability, confirming its inherent cytotoxic potential. However, the overall reduction remained moderate, likely due to limited intracellular uptake in the absence of delivery-enhancing mechanisms.

When ultrasound was combined with dFdC HCl (blue bars), a notable enhancement in cytotoxicity was observed compared to drug alone. At mid ultrasound intensity, cell viability decreased from 68% to 55% at  $5 \,\mu g/mL$ , from 66% to 50% at  $10 \,\mu g/mL$ , and from 51% to 49% at  $15 \,\mu g/mL$ . These results suggest that ultrasound-mediated sonoporation improves membrane permeability and facilitates greater drug uptake.

However, when microbubbles were added to the dFdC HCl + ultrasound treatment (green bars), no significant additional reduction in viability was observed under mid-intensity ultrasound. For instance, at  $10 \,\mu g/mL$ , viability only declined slightly from 66% (dFdC HCl alone) to 64% (dFdC HCl + ultrasound + microbubble), indicating minimal enhancement from microbubbles at this intensity level.

Overall, mid-intensity ultrasound significantly enhanced the cytotoxic effect of dFdC HCl, though the addition of microbubbles did not further amplify this effect under the tested conditions.

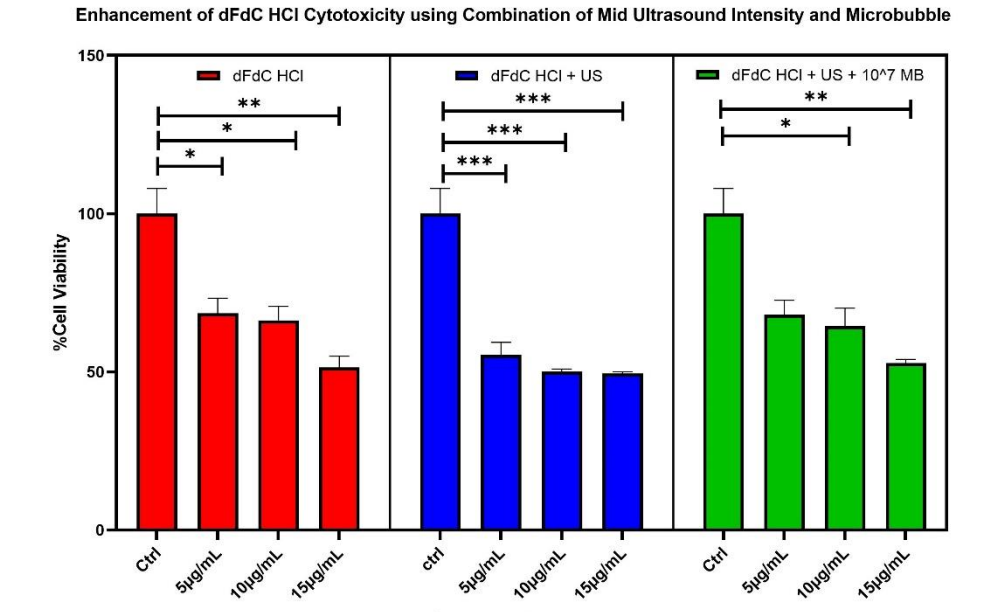


Figure-14: Effect of dFdC HCl on cell viability under three conditions: dFdC HCl alone (red), dFdC HCl + mid ultrasound intensity (blue), and dFdC HCl + mid ultrasound intensity +  $10^7$  microbubbles (green). All groups show dose-dependent cytotoxicity, with enhanced effects in ultrasound and microbubble-assisted treatments, indicating improved drug delivery via sonoporation. Data are expressed as mean  $\pm$  SE (N=3), (\*p<0.05), (\*\*p<0.005), (\*\*\*p<0.0001).

Concentration in µg/mL

# 4.6 Enhanced Cytotoxicity of dFdC HCl via Combined High Intensity Ultrasound with Microbubbles

**Figure 15** illustrates the effects of dFdC HCl treatment alone and in combination with high-intensity ultrasound on MIA PaCa-2 cell viability. The experimental groups mirrored those used in the midintensity setup.

Treatment with dFdC HCl alone (red bars) resulted in a clear dose-dependent reduction in viability, decreasing to 53% at 5  $\mu$ g/mL and 50% at 15  $\mu$ g/mL, confirming the drug's intrinsic cytotoxicity. When combined with high-intensity ultrasound (blue bar), viability further declined to 45% at 15  $\mu$ g/mL, suggesting that ultrasound-induced

sonoporation enhances membrane permeability and facilitates increased intracellular drug uptake.

The most pronounced reduction in viability was observed in the group receiving the combined treatment of dFdC HCl, ultrasound, and microbubbles (green bars). Under high-intensity ultrasound, viability dropped from 52% to 49% at 10 µg/mL, and from 50% to 43% at 15 µg/mL. This enhanced cytotoxicity is likely attributable to the cavitation effects of microbubbles, which intensify ultrasound-mediated membrane disruption and promote greater intracellular accumulation of dFdC HCl. Additionally, mechanical stress from cavitation may contribute to further cellular damage, amplifying the overall cytotoxic effect.

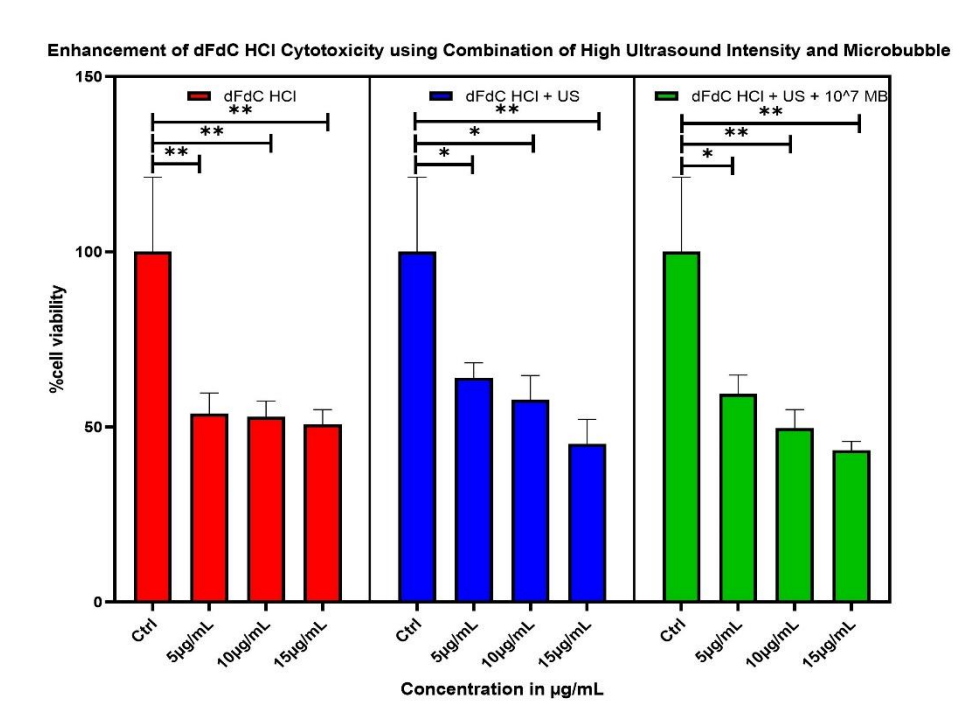


Figure 15: Effect of dFdC HCl on cell viability under three conditions: dFdC HCl alone (red), dFdC HCl + high ultrasound intensity (blue), and dFdC HCl + high ultrasound intensity +  $10^7$  microbubbles (green). All groups show dosedependent cytotoxicity, with enhanced effects in ultrasound and microbubble-assisted treatments, indicating improved drug delivery via sonoporation. Data are expressed as mean  $\pm$  SE (N=3), (\*p<0.05), (\*\*p<0.005).

### Chapter 5

### **Summary and Future Prospectives**

This study systematically evaluated the cytotoxic and membrane-permeabilizing effects of dFdC HCl on MIA PaCa-2 pancreatic cancer cells, both as a standalone treatment and in combination with ultrasound and microbubbles, using MTT assays and fluorescence imaging to evaluate the cellular uptake EtDH-1.

The MTT assay demonstrated a clear dose-dependent reduction in cell viability with increasing concentrations of dFdC HCl (1–15  $\mu$ g/mL), with viability dropping to approximately 51% at the highest dose. This indicates that while the drug is inherently cytotoxic, its effect may be limited by suboptimal cellular uptake.

Fluorescence microscopy using calcein AM and EtHD-1 further confirmed minimal membrane disruption in control, with a modest increase in cell death observed with ultrasound alone. The addition of microbubbles significantly enhanced ultrasound-induced membrane disruption, especially at mid ultrasound intensity combined with a high microbubble concentration (10<sup>7</sup> microbubbles), as reflected by increased EtHD-1 uptake. At high ultrasound intensity, a strong permeabilization effect was observed even without microbubbles, likely due to direct mechanical stress; however, the combination with microbubbles at this intensity showed slightly reduced EtHD-1 uptake, suggesting possible microbubble collapse or destabilization under excessive acoustic pressure.

Microbubble characterization revealed a narrow size distribution centred around  $7 \, \mu m$ , ideal for stable cavitation and effective vascular navigation, which likely contributed to the reproducibility and efficiency of ultrasound-mediated delivery in this study. The viability data from MTT assays aligned with these observations, ultrasound or microbubble treatment alone induced only mild cytotoxic effects ( $\sim 85\%$  viability), confirming good biocompatibility. However, the combination (ultrasound + microbubble) slightly reduced viability ( $\sim 80\%$ ),

suggesting that mechanical effects of sonoporation modestly impact cell health while remaining within tolerable limits for therapeutic application.

In the dFdC HCl uptake experiments, the combination of dFdC HCl with ultrasound and microbubbles demonstrated a synergistic effect in enhancing cytotoxicity. Under mid ultrasound intensity, the triple treatment yielded no further improvements compared to only midintensity ultrasound, whereas under high ultrasound intensity, a significant drop in viability was observed indicating improved drug delivery and amplified intracellular effects. The highest efficacy was achieved with the highest drug concentration combined with microbubble and high Ultrasound intensity, resulting in ~43% cell viability, compared to ~51% for drug alone, and ~45% for drug with high Ultrasound alone.

Overall, these findings confirm that high-intensity ultrasound with and without ultrasound can substantially enhance the delivery and efficacy of chemotherapeutic agents like dFdC HCl through controlled membrane permeabilization

For future work optimization of ultrasound parameters and microbubble concentrations is essential for maximizing therapeutic outcomes while maintaining cell viability within an acceptable range, making this a promising strategy for targeted cancer treatment via sonoporation.

Further enhancement of therapeutic potential of ultrasound- and microbubble-mediated drug delivery, future research should focus on:

- 1. **Optimization of Acoustic Parameters**: Systematic evaluation of ultrasound intensity, frequency, pulse duration, and duty cycle to identify optimal values that favor stable cavitation without compromising microbubble integrity.
- 2. **Microbubble Engineering**: Exploring novel microbubble formulations with enhanced stability, targeted surface ligands, or

- drug-loading capabilities to improve delivery efficiency and specificity.
- 3. **Advanced Assays**: Incorporating more sensitive and mechanistic assays (e.g., flow cytometry, real-time imaging, and apoptosis markers) to better assess cellular responses and identify optimal therapeutic windows.
- 4. **Combination Therapies**: Investigating the synergistic effects of sonoporation with other modalities, such as immunotherapy or radiotherapy, to potentiate antitumor responses.
- 5. *In Vivo* Validation: Extending these findings to *in vivo* models to evaluate therapeutic efficacy, biodistribution, and safety under physiologically relevant conditions.

Ultimately, fine-tuning sonoporation-based delivery systems could lead to more effective, localized, and minimally invasive strategies for pancreatic cancer treatment and beyond.

### References

- [1] I. Ilic and M. Ilic, "International patterns in incidence and mortality trends of pancreatic cancer in the last three decades: A joinpoint regression analysis," *World J Gastroenterol*, vol. 28, no. 32, pp. 4698–4715, Aug. 2022, doi: 10.3748/wjg.v28.i32.4698.
- [2] A. Y. Bazeed, C. M. Day, and S. Garg, "Pancreatic Cancer: Challenges and Opportunities in Locoregional Therapies," *Cancers (Basel)*, vol. 14, no. 17, p. 4257, Aug. 2022, doi: 10.3390/cancers14174257.
- [3] C. M. I. Quarato *et al.*, "A Review on Biological Effects of Ultrasounds: Key Messages for Clinicians," Mar. 01, 2023, *Multidisciplinary Digital Publishing Institute (MDPI)*. doi: 10.3390/diagnostics13050855.
- [4] F. E. Shamout *et al.*, "Enhancement of Non-Invasive Trans-Membrane Drug Delivery Using Ultrasound and Microbubbles During Physiologically Relevant Flow," *Ultrasound Med Biol*, vol. 41, no. 9, pp. 2435–2448, Sep. 2015, doi: 10.1016/j.ultrasmedbio.2015.05.003.
- [5] H. Yu, Z. Lin, L. Xu, D. Liu, and Y. Shen, "Theoretical study of microbubble dynamics in sonoporation," *Ultrasonics*, vol. 61, pp. 136–144, Aug. 2015, doi: 10.1016/j.ultras.2015.04.008.
- [6] A. G. Sorace, J. M. Warram, H. Umphrey, and K. Hoyt, "Microbubble-mediated ultrasonic techniques for improved chemotherapeutic delivery in cancer," *J Drug Target*, vol. 20, no. 1, pp. 43–54, Jan. 2012, doi: 10.3109/1061186X.2011.622397.
- [7] A. Upadhyay and S. V. Dalvi, "Microbubble Formulations: Synthesis, Stability, Modeling and Biomedical Applications," Feb. 01, 2019, *Elsevier USA*. doi: 10.1016/j.ultrasmedbio.2018.09.022.
- [8] P. S. Epstein and M. S. Plesset, "On the stability of gas bubbles in liquid-gas solutions," *J Chem Phys*, vol. 18, no. 11, pp. 1505–1509, 1950, doi: 10.1063/1.1747520.
- [9] D. Omata, J. Unga, R. Suzuki, and K. Maruyama, "Lipid-based microbubbles and ultrasound for therapeutic application," *Adv Drug Deliv Rev*, vol. 154–155, pp. 236–244, 2020, doi: 10.1016/j.addr.2020.07.005.
- [10] Sirsi S, Borden M. Microbubble Compositions, Properties and Biomedical Applications. Bubble Sci Eng Technol. 2009 Nov;1(1-2):3-17. doi: 10.1179/175889709X446507.
- [11] Przystupski D, Ussowicz M. Landscape of Cellular Bioeffects Triggered by Ultrasound-Induced Sonoporation. Int J Mol Sci. 2022 Sep 23;23(19):11222. doi: 10.3390/ijms231911222.
- [12] Y. Yang, Q. Li, X. Guo, J. Tu, and D. Zhang, "Mechanisms underlying sonoporation: Interaction between microbubbles and cells," *Ultrason Sonochem*, vol. 67, p. 105096, Oct. 2020, doi: 10.1016/j.ultsonch.2020.105096.

- [13] I. Lentacker, I. De Cock, R. Deckers, S. C. De Smedt, and C. T. W. Moonen, "Understanding ultrasound induced sonoporation: Definitions and underlying mechanisms," *Adv Drug Deliv Rev*, vol. 72, pp. 49–64, Jun. 2014, doi: 10.1016/j.addr.2013.11.008.
- [14] Liu, Y., Cho, CW., Yan, X. *et al.* Ultrasound-Induced Hyperthermia Increases Cellular Uptake and Cytotoxicity of P-Glycoprotein Substrates in Multi-Drug Resistant Cells. *Pharm Res* **18**, 1255–1261 (2001). https://doi.org/10.1023/A:1013025625156
- [15] Ł. Fura, R. Tymkiewicz, and T. Kujawska, "Numerical studies on shortening the duration of HIFU ablation therapy and their experimental validation," *Ultrasonics*, vol. 142, p. 107371, Aug. 2024, doi: 10.1016/j.ultras.2024.107371.
- [16] Y. Qiu, C. Zhang, J. Tu, and D. Zhang, "Microbubble-induced sonoporation involved in ultrasound-mediated DNA transfection in vitro at low acoustic pressures," *J Biomech*, vol. 45, no. 8, pp. 1339–1345, May 2012, doi: 10.1016/j.jbiomech.2012.03.011.
- [17] D. L. Miller, N. B. Smith, M. R. Bailey, G. J. Czarnota, K. Hynynen, and I. R. S. Makin, "Overview of therapeutic ultrasound applications and safety considerations," *Journal of Ultrasound in Medicine*, vol. 31, no. 4, pp. 623–634, Apr. 2012, doi: 10.7863/jum.2012.31.4.623.
- [18] N. M. Al Sawaftah and G. A. Husseini, "Ultrasound-mediated drug delivery in cancer therapy: A Review," *J Nanosci Nanotechnol*, vol. 20, no. 12, pp. 7211–7230, Jul. 2020, doi: 10.1166/jnn.2020.18877.
- [19] A. A. Doinikov and A. Bouakaz, "Acoustic microstreaming around a gas bubble," *J Acoust Soc Am*, vol. 127, no. 2, pp. 703–709, Feb. 2010, doi: 10.1121/1.3279793.
- [20] Postema, Michiel & Kotopoulis, Spiros & Delalande, Anthony & Gilja, Odd. (2012). Sonoporation: Why Microbubbles Create Pores. Ultraschall in der Medizin. 33. 97-98. 10.1055/s-0031-1274749.
- [21] M. Ward, J. Wu, and J.-F. Chiu, "Experimental study of the effects of optison® concentration on sonoporation in vitro," *Ultrasound Med Biol*, vol. 26, no. 7, pp. 1169–1175, Sep. 2000, doi: 10.1016/S0301-5629(00)00260-X.
- [22] Y.-Z. Zhao *et al.*, "Phospholipids-based microbubbles sonoporation pore size and reseal of cell membrane cultured *in vitro*," *J Drug Target*, vol. 16, no. 1, pp. 18–25, Jan. 2008, doi: 10.1080/10611860701637792.
- [23] Charles A. Kelsey PhD, "Biological effects of ultrasound," in *radiation biology of medical imaging*, Wiley, 2014, pp. 269–280. doi: 10.1002/9781118517154.ch16.
- [24] B. Baseri, J. J. Choi, Y.-S. Tung, and E. E. Konofagou, "Multi-modality safety assessment of Blood-Brain Barrier opening using focused ultrasound and definity microbubbles: A Short-term Study," *Ultrasound Med Biol*, vol. 36, no. 9, pp. 1445–1459, Sep. 2010, doi: 10.1016/j.ultrasmedbio.2010.06.005.

- [25] W. Lim Kee Chang *et al.*, "Rapid short-pulses of focused ultrasound and microbubbles deliver a range of agent sizes to the brain," *Sci Rep*, vol. 13, no. 1, p. 6963, Apr. 2023, doi: 10.1038/s41598-023-33671-5.
- [26] S. V. Morse *et al.*, "Rapid short-pulse ultrasound delivers drugs uniformly across the murine Blood-Brain Barrier with negligible disruption," *Radiology*, vol. 291, no. 2, pp. 459–466, May 2019, doi: 10.1148/radiol.2019181625.